

Optimum Deposition of Tungsten Oxide on Titania Nanotubular Arrays and Study the Photoactivity of Nano-Composite Photoanode

Asma Mustafa Husin Milad^{1*}, Soud Saad Awitil², Mohammad B. Kassim³, Wan Ramli Wan Daud⁴

¹ asma.aga2009@gmail.com, ² soudsaad177@gmail.com, ³ mb_kassim@ukm.edu.my,
⁴ wramli@eng.ukm.my

^{1,2} Department of Chemical & Petroleum Engineering, College of Engineering, Elmergib University, Libya

³ School of Chemical Sciences and Food Technology, Faculty of Science and Technology, UKM, Bangi, Malaysia

⁴ Department of Chemical & Process Engineering, Faculty of Engineering & Built Environment, UKM, Bangi, Malaysia

*Corresponding author email: asma.aga2009@gmail.com

Received: 00 April 2018 / Accepted: 00 May 2018

ABSTRACT

The novelty of this research works in the two-step formation of tungsten oxide (WO₃)-loaded TiO₂ nanotube arrays composite film by study the optimum conditions of electrodeposition of WO₃ nanoparticles on TiO₂ nanotubes arrays based on their photo-activity performance. The W have been incorporated from a sodium tungstate-based aqueous electrolyte containing from 0.2 M sodium tungstate (Na₂WO₄) with addition of 0.13 M hydrogen peroxide (30%) and drops from H₂SO₄ up to get pH = 1; it accumulates to form a self independent structure of WO₃ on the surface of the nanotubes. WO₃ was deposited for several times intervals at room temperature and annealed at 350 °C for 30 minutes. TiO₂ nanotubes (TNTA) were successfully grown by anodizing of titanium foil (Ti) in organic (98% vol., ethylene glycol, 2 vol.% Di water and 0.5 wt% ammonium fluoride and acidic (0.5M phosphoric acid and 0.14M sodium fluoride) electrolyte. The possible growth of TiO₂ nanotubes in the applied potential at 20V for 45 minutes was investigated. It were found such electrochemical condition resulted in formation of nanotube with average diameter 50 & 120 nm and the length 3.5 & 0.6 μm for organic and acidic electrolytes respectively. The anodized samples were annealed at 500 °C in N₂ gas for 3 hours. The structural, morphology and composition of TiO₂ nanotubes and WO₃/TiO₂ nanotube were characterized with XRD, FESEM and EDX. FESEM results of the nanotubular arrays showed uniform arrays of titania nanotubular and showed. EDX results showed trace of tungsten has been incorporated into TiO₂. The influences of tungsten content on the photocurrent densities of WO₃/TiO₂ nanotubular photoanodes were investigated by recording current-potential profiles. The preliminary results indicated that the WO₃/TiO₂ produced showed good photocurrent densities due to the behavior of W⁶⁺ ions which allows to electron traps that suppress electron-hole recombination and exploit the lower band gap of material to produce a water splitting process by increasing the charge separation and extending the energy range of photo-excitation for the system.

Keywords: Titanium oxide nanotubular arrays (TNT), Anodization, tungsten oxide (WO₃), electrodeposition, photoelectrochemical measurements.

1 Introduction

Hydrogen is an attractive alternative source of energy because it is renewable if collected through the splitting of water, burns cleanly (producing only H₂O), and could deliver energy in the same method as fossil fuels, via combustion or electricity through the use of fuel cells. Generated hydrogen through the splitting of water is a very desirable alternative fuel for the following reasons: sunlight is a plentiful and renewable energy source [1]; the hydrogen generating device has no moving parts, therefore maintenance is minimal; and the associated infrastructure is simple [2]. Photoelectrochemical reaction for water splitting is a process in which water is split into hydrogen (H₂) and oxygen (O₂) on the surface of a specific type of photoactive material, namely titania (TiO₂) semiconductor [3, 4]. The photocatalytic splitting of water using oxide semiconductors is initiated by the direct absorption of a photon, which creates separated electrons and holes in the energy band gap of the material [5]. During the past few decades, significant efforts have been made to search for a low cost and efficient photoelectrochemical cell (PEC). An ideal PEC cell needs to have an optimum band gap with the right band positions for both its CB and VB. In addition, it needs to be readily available, non-toxic and stable in an aqueous solution. Moreover, this material has to have a high absorption and good photon-to-electron conversion efficiency. So far, no single material has been found that meets all the criteria above for a cheap and efficient PEC cell. Most of the existing materials suffer from either stability issues or low photon-to-electron conversion efficiency. TiO₂ has high band gap level which has a potential for water splitting under UV-light, but it cannot absorb visible light and hence, suffer from low light absorption efficiency. An anatase TiO₂ shows fewer recombination reactions due to the indirect band gap and hence, produces better photocatalytic activity compared to rutile that has a direct band gap. Moreover, other oxide such as WO₃ has low band gap level of 2.2-2.8 eV [6] has good absorbance in visible light but it has insufficient CB or VB edge for water reduction and oxidation; it can absorb the blue region of the solar spectrum up to ca. 500 nm. Recently, WO₃ was considered as a new photoanode material or mixture material with TiO₂ for water splitting because WO₃ can offer relatively small band gap and has high stability in an aqueous solution. Although WO₃ has shown great potential such as photo-oxidation of water with visible light and has high photocurrent levels with nanocrystals, the quantum yield is still low [7, 8]. In this work, strategies were centred on controlling the structure or the chemical composition of the TiO₂ nanotube arrays composite (TNTA). The electrochemical anodization is the simplest method of fabricating TNTA from a titanium foil. The 1-D nanostructures offer highly efficient charge transport channels longitudinally. Various efforts have been made to employ mixed WO₃/TiO₂ systems to enhance the efficiency of electrochromic effects in aqueous solution [9, 10]. Whereas, the enhancement of the photocatalytic performances of TiO₂ was possible since WO₃ can serve as an electron accepting species [11]. However, WO₃/TiO₂ or WO_x/TiO₂ were mainly prepared by different methods as physical mixing [12], multi-step grafting of ammonium tungstate [13, 14], improved sol-gel method, co-precipitation [15], hydrothermal method [16] and electrodeposition [17], where WO₃ or WO_x only covered the surface of TiO₂ with low amounts in most situations. The ability of WO_x-TiO₂ to be excited by visible light and degrade the dyes were confirmed by several researchers, where Li et al. (2001) proven that the photoactivity of WO_x-TiO₂ was significantly higher than that of pure TiO₂ and an optimal content of WO_x in TiO₂ was found to be 3% for WO_x in TiO₂ was the highest rate of methylene blue (MB) photodegradation [18]. The most related researches about WO₃/TiO₂ were summarized in Table 1.

Table 1: Summary of previous researches about Tungsten trioxide on TNTA

	Synthesis Method	Significant Findings	Ref
WO₃/TNTA nanocomposite	Electrochemical deposition	The maximum conversion efficiency of 0.87% was obtained for WO ₃ /TNTA nano-composite. H ₂ and O ₂ gases were collected during the photoreaction were had the volume ratio of 2.2:1 volume ratio.	[19]
W-Doped TNTA	A direct anodization	Showed that photocurrent densities of 3 wt% W-doped TNTA which were obtained were 0.25 mA/cm ² at 1 V bias, which is much higher than that of the undoped sample.	[20]
WO₃/TNTA nanocomposite	A facile hydrothermal method	Exhibited enhanced photocatalytic activity toward Rhodamine B (RhB) degradation when compared with pure TNTA and P25. The optimum percentage of WO ₃ decorated on TNTA for the improvement of photocatalytic properties is 5 wt. %.	[21]
WO₃-TNTA	A sol-gel template technique	Samples exhibited a strong photoresponse in the visible region and a low PL emission. High efficiency of 2,3-dichlorophenol degradation was obtained under visible light.	[22]
W doped TNTA	An anodization of Ti-W alloys	The content of 9 at% WO ₃ in photoresponse experiments is most beneficial, in long term experiments a higher efficiency is observed for the 0.2 at% W content.. This demonstrates that under optimized WO ₃ doping conditions a lasting visible light activation of TiO ₂ nanotubes can be achieved.	[23]
W-TNTA	A radio-frequency (RF) sputtering	The effect of W on the photoelectrochemical properties of TNTA was due to W atoms which occupy the substitutional position within the vacancies of TNTA. Found the W-TNTA system plays important roles in efficient electron transfers due to the reduction in e ⁻ /h ⁺ recombination.	[24]
WO₃-TNTA	A wet impregnation	A maximum photocurrent of 2.1 mA/cm ² with a photoconversion efficiency of 5.1% was obtained, which is approximately twice higher than that of pure TiO ₂ nanotubes. The findings were mainly attributed to higher charge carrier separation, which minimized the recombination losses and enhanced the transportation of photo-induced electrons in this binary hybrid photoelectrode.	[25]
WO₃-TNTA	A wet impregnation	A low content of WO ₃ species successfully diffused into the TiO ₂ lattice and formed W-O-Ti bonds, which significantly promoted effective charge separation by trapping photo-induced electrons from TiO ₂ . The photocurrent density, photoconversion efficiency, STH efficiency, and H ₂ generation of the resultant hybrid nanotubes were increased.	[26]
WO₃-TNTA	A wet impregnation	In PEC studies, high-crystallinity anatase-phase WTNs exhibited a higher photocurrent density (2.4 mA/cm ²) than WTNs of amorphous or polycrystalline phases.	[27]
WO₃/TiO₂ heterojunction	Liquid phase deposition	TiO ₂ film provides an excellent platform for WO ₃ deposition. WO ₃ expands the absorption band edge of TiO ₂ film to visible light region. WO ₃ /TiO ₂ heterojunction film shows high photoelectrocatalytic activity.	[28]
WO₃-loaded TiO₂ nanotube	Tungsten as the cathode	WO ₃ -loaded TiO ₂ nanotube arrays with the highest aspect ratio, geometric surface area factor and at% of tungsten exhibited the more favorable photocatalytic degradation of MO dye under UV light irradiation	[29]

As a result, the main focus of this work is to enhance the photocurrent density of TNTA and increased its ability to generate hydrogen by deposition of WO₃ nanoparticles and to form a highly efficient nanocomposite structure. As well, the optimum conditions of electrodeposition of WO₃ on TNTA to get the best photocurrent of TNTA semiconductors in PEC. A full investigation of the intrinsic material properties of the resulted samples was performed, which included crystallinity, morphology, and electronic absorption spectrum, by FESEM, X-ray diffraction (XRD) and UV-VIS diffuse reflectance. Finally the optimised photoelectrodes were investigation by measuring photocurrents enhancement via PEC measurements.

2 Materials and Methods

Short TiO₂ nanotubular array (STNTA) was prepared by anodizing a Ti-foil in **an acidic electrolyte** [30] containing 0.5M *ortho*-phosphoric acid and 0.14M sodium fluoride at pH 2 under constant stirring and the voltage profile. Similarly, a much longer titania nanotubes were synthesized in accordance with the procedures reported by [31]) which required the anodization of T-foil in an **organic electrolyte** consisting of ethylene glycol (EG) with 2% vol. DI water and 0.3 wt% of NH₄F at pH 5.9. The post-treatment process of the TNTA prepared above involved annealing, which is a vital step for the transformation of the amorphous state of titanium oxide into anatase crystals. Prior to annealing, the surface of the anodized samples was cleaned with deionized water to remove ionic residues, and the samples were dried under N₂ flow at 100 °C for 12 hr. The TNTA samples were loaded in to a muffle furnace in a ceramic boat and were annealed at 500 °C for 3 hr in N₂ flow. The temperature was increased at a rate of 5 °C/min. The synthetic procedures for making Tungsten Oxide/TNTA were improved from previously reported work through few modifications such as deposition bath compositions, calcination temperature and electrodes configurations as summarized in Table 2. However, Figure 1 shows the cyclic voltammetry scan of TNTA in deposition electrolyte, whereas, the cyclic voltammogram suggested that the electrodeposition potential of about -0.38 V which is similar to the reported potential for W(IV) reduction to W(0) [32].

Table 2 : *Electrodeposition and calcinations conditions of tungsten oxide on TNTA electrodes.*

Electrodeposition Bath	Deposition Temperature	Electrodes Configuration	Calcination Conditions	Ref.
<ul style="list-style-type: none"> • 0.2M of Sodium tungstate (Na₂WO₄, 99%, Merck) • 0.13M of Hydrogen Peroxide Solution (H₂O₂, 30%, Sigma-Aldrich)₂ and • drops of Sulfuric acid (H₂SO₄, 70%, Merck) 	23-25 °C	Anode: Long-TNTA (LTNTA) & Short-TNTA (STNTA) Cathode:Pt Reference: Ag/AgCl	350 °C for 30 min in purified air	Krasnov and Kolbasov [33]

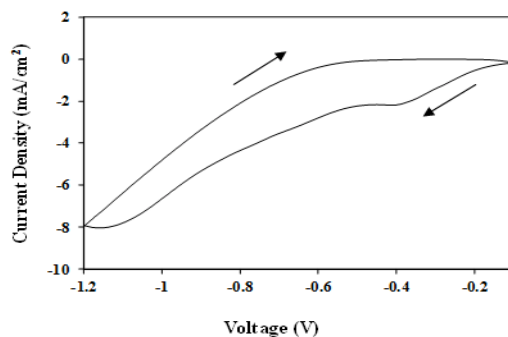


Figure 1: Cyclic voltammogram of TNTA electrode in 0.2M Na_2WO_4 , 0.13M H_2O_2 electrolyte.

The synthesized photoanodes were characterized by field emission scanning electron microscope (FESEM), energy dispersive X-ray (EDX), X-ray photoelectron spectrometer (XPS), X-ray diffraction (XRD) and ultraviolet and visible light (UV-VIS) spectroscopy. Photoelectrochemical data of the photoanodes were collected by using the in-house PEC system [34, 35] and the results were discussed in comparison with TNTA.

3 Results and Discussion

Figure 2 and Figure 3 show the morphology (FESEM top-view) of the STNTA and LTNTA with WO_3 deposit, respectively. It can be seen that TiO_2 tubes are covered with a very thin layer of WO_3 started to form and became much thicker as the deposition period became longer (Figure 2c and 3c). However, in most cases the surface area shows open and nicely decorated tubes with small individual WO_3 nanoparticles (diameter of ~ 5 nm) was visible for 5 minutes deposition period and became larger (agglomeration) as the deposition time getting longer until a thick layer was formed as shown in Figure 2e & f and 3f. The EDX result is represented and it clearly indicates that W is present (Table 3) in the particles.

Table 3: Elemental Composition of WO_3 /TNTA at different deposition periods.

Deposition Time (min)	Elemental content (Atomic %)							
	WO_3 /STNTA				WO_3 /LTNTA			
	Ti	O	C	W	Ti	O	C	W
1	35.38	64.57	-	0.04	41.69	51.08	7.13	0.11
5	37.96	61.88	-	0.16	37.07	59.09	3.61	0.23
10	38.69	61.05	-	0.26	28.89	57.02	13.82	0.28
15	57.41	42.19	-	0.40	26.55	55.32	17.68	0.45
30	51.26	47.73	-	1.01	30.72	59.61	9.01	0.66
45	32.60	60.58	-	6.823	26.45	65.04	5.77	2.74

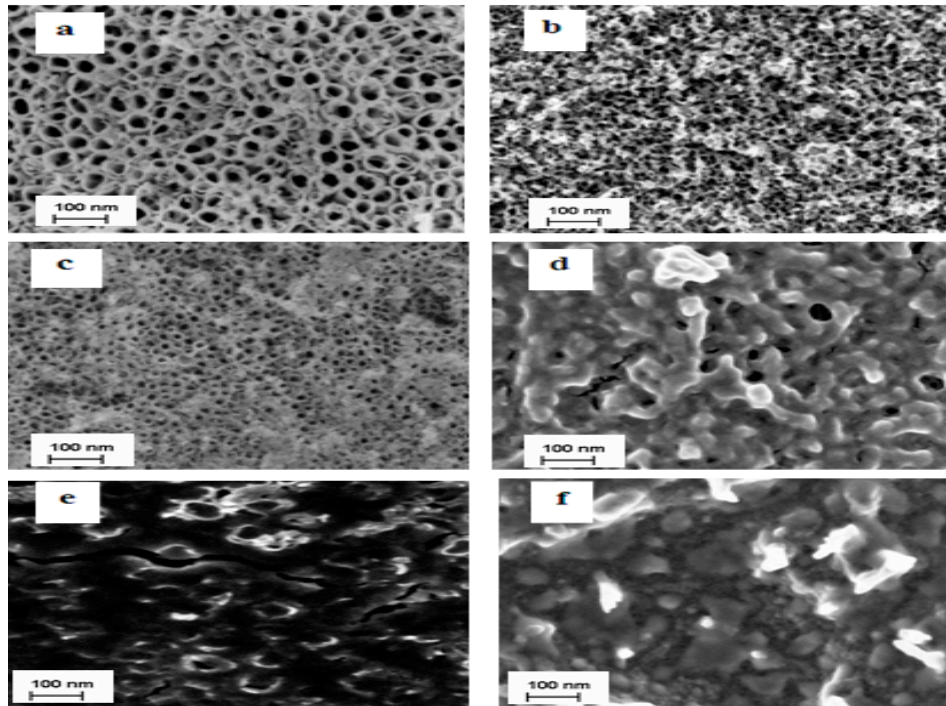


Figure 2: FESEM top view of $WO_3/STNTA$ at variety deposition time: (a) 1, (b) 5, (c) 10, (d) 15, (e) 30, and (f) 45 minutes.

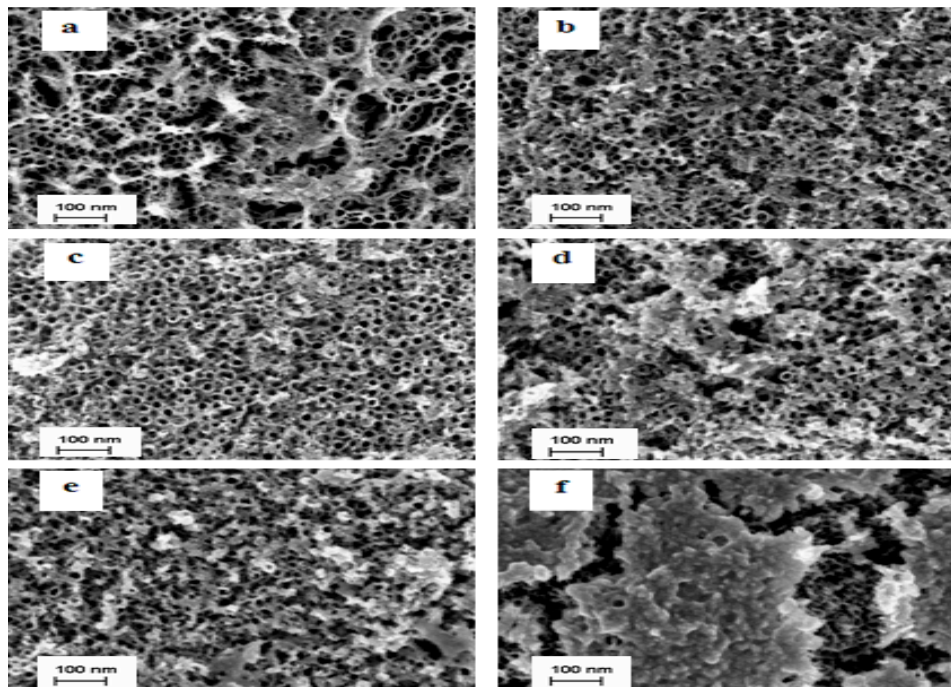


Figure 3: FESEM top view of $WO_3/LTNTA$ at selection deposition time: (a) 1, (b) 5, (c) 10, (d) 15, (e) 30, and (f) 45 minutes.

For WO_3 -TNTA nanocomposite electrode, the content existences of deposited WO_3 nanoparticles on short and long TNTA were studied by XRD measurement. The XRD patterns for WO_3 -STNTA and WO_3 -LTNTA are depicted in Figure 4a & b, respectively. Previous investigations on bulk WO_3 have reported the following phase transformation sequence upon heating: triclinic (δ - WO_3) (-30°C) \rightarrow monoclinic (γ - WO_3) (330°C) \rightarrow orthorhombic (β - WO_3) (740°C) \rightarrow tetragonal (α - WO_3) [36]. In this work, the XRD patterns (Figure 4a & b) show diffraction signals for the monoclinic WO_3 under the conditions (JCPDS No.83-950), indicating a desirable crystallinity was formed in the nanocomposite sample after calcinations at 350°C [37]. As shown in Figure 4a & b, there was no new diffraction peak can be ascribed to the crystal phase of $\text{W}_x\text{Ti}_{1-x}\text{O}_2$ for the calcination temperatures used in this study which can be concluded that no reaction between oxides. The nanocomposite show sharp diffraction peaks at 34.0° (202), 49.0° (004), and 55.3° (024), for WO_3 /LTNTA's XRD spectrum which were similar to those detected by Lai and Sreekantan [25].

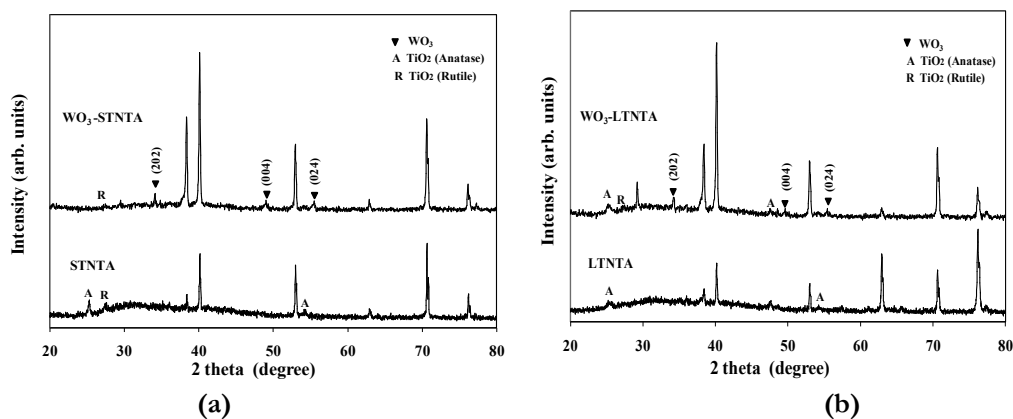


Figure 4: X-ray diffraction patterns of (a) WO_3 /STNTA and (b) WO_3 /LTNTA.

However, the peak at 30° was unknown. The XRD profiles of WO_3 /LTNTA became stronger and sharper than WO_3 /STNTA because most of the deposited WO_3 nanoparticles were formed on the surface of the LTNTA (due to smaller tube diameter) but the particles were deposited in the tubes and on the surface (due to big diameter) of the STNTA. The reflectance ($R\%$) of WO_3 /TNTA nanocomposites were measured using UV-VIS spectroscopy, and the reflectance spectra are shown in Figure 5. The transmittances were almost zero due to the Ti base. The intensity of the reflectance depends on the morphology and amount of metal oxide formed on the surface. Besides absorption by the deposited nanoparticles, the detected scattering of light was very weak due to the morphological structure of tubes which absorbs the scattering light. The fluctuation of reflectance was strong in 1- WO_3 /TNTA samples in the visible region (400 to 800 nm) for one min deposition period as shown in Figure 6. This is due to the small amount of WO_3 content. The WO_3 /TNTAs with different WO_3 contents were used as photoelectrodes in PEC water-splitting cell for evaluation of their photocurrent densities production. The photocurrent density-voltage response was plotted under 100 W/m^2 illuminations. The corresponding experimental results are presented in Figure 6a & b for WO_3 /TNTA and WO_3 /TNTA respectively for different deposition periods. The maximum photocurrent densities of 0.3 and 0.37 mA/cm^2 were observed at 1 V vs. SCE in the 10- WO_3 /STNTA and 15- WO_3 /LTNTA with 0.16 and 0.45 at% of W content respectively, which is relatively higher

compared with that of the pure STNTA and LTNTA (0.06 and 0.32 mA/cm² at 1 V vs. SCE, respectively). The WO₃/STNTA prepared by deposition for 1, 5, 15, 30 and 45 min exhibited decreased photocurrent densities of approximately 0.1, 0.18, 0.17, 0.14 and 0.12 mA/cm² at 1 V vs. SCE, respectively. It is noted that WO₃/LTNTA photoanodes which were deposited for 1, 5, 10, 30 and 45 min produced photocurrent densities about 0.19, 0.26, 0.33, 0.22 and 0.09 mA/cm² at 1 V vs. SCE, respectively. These results clearly showed the significant effects of different WO₃ contents in the TNTA on the PEC performances. The resultant photocurrent densities of WO₃/STNTA increased linearly as shown in Figure 6a. Moreover in Figure 6b, the photocurrent densities of WO₃/LTNTA at 1, 15 and 45 min deposition periods were mostly constant, and the other curves were increased slightly in logarithmic shape.

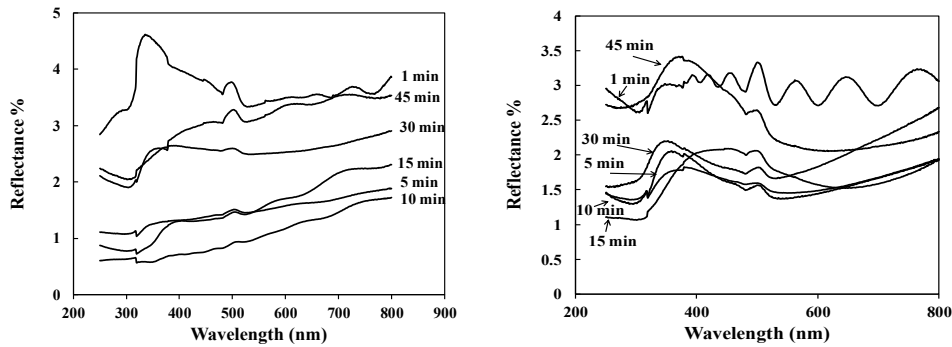


Figure 5: Reflectance spectra of WO₃/STNTA (left) and WO₃/LTNTA (right) at various deposition periods.

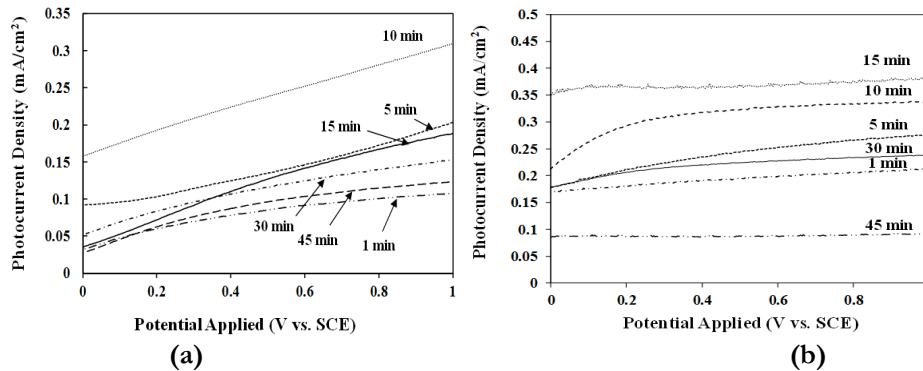


Figure 6: Photocurrent density as a function of measured potential (vs. SCE) for a) WO₃/STNTA and b) WO₃/LTNTA photoelectrodes deposited at different deposition period under light illumination.

Figure 7 was illustrated the predicted mechanism of electrons movement in WO₃/TNTA photoelectrodes. Composite WO₃ and TNTA materials have shown a favorable electron injection from the CB of TNTA to that of WO₃ and hole transfer between VBs in the opposite direction, which reduces e⁻/h⁺ recombination in both semiconductors. The CB of WO₃ is not negative enough for water reduction, some modifications are needed to achieve H₂ evolution. Also WO₃/TNTAs have a higher UV response compared to WO₃ materials. This is improvement could be attributed in part to better absorption and better transport due to the organized nanostructures. In addition, the electron transfer from TNTA to WO₃ results in a wide electron-hole separation, which could improve the IPCE values as well

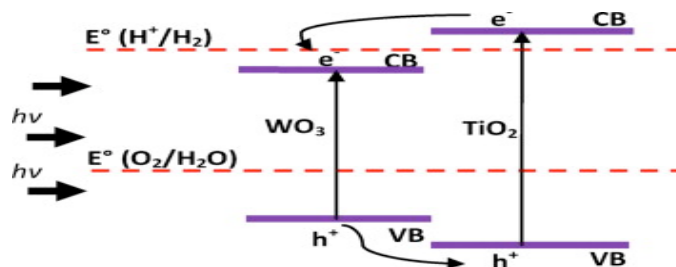


Figure 7: Schematic diagram showing the energy band position and the electron transfer direction for WO_3 /TNTA nanocomposite electrode after being excited by light.

4 Conclusion

This work was focused on the synthesis, characterization, PEC testing of hetero-nanocomposite TNTA semiconductors with WO_3 nanoparticles. However, getting the best performance for the photoelectrochemical testings for electrodes were quite difficult since it was influenced by the stability and the ability of the electrodes to produce photocurrent. However, short and long TNTA synthesized by anodization of Ti-foil in two types of electrolytes (acidic and organic) lead to synthesis two different morphologies of TNTA. Subsequently, Metal oxides nanoparticles (WO_3) which has a small band gap were deposited on TNTA individually from sodium tungstate aqueous solution at room temperature. The morphologies of deposited WO_3 on TNTA varied depending on deposition periods and crystal type. Similarly, the content of WO_3 on TNTA increased upon electrodeposition period according to EDX results. Likewise, for WO_3 /STNTA and WO_3 /LTNTA the maximum photocurrent were 0.3 mA at 10 minutes and 0.37 mA at 15 minutes, respectively.

5 Acknowledgment

The authors express their sincere thanks to Universiti Kebangsaan Malaysia for allowing this work to use the UKM-GUP-BTT-07-30-190, UKM-OUP-TK-16-73/2010 and UKM-OUP-TK-16-73/2011 research grants. A.M.H. Milad thanks the Elmergib University.

6 References

- [1] M. Gratzel. "Photoelectrochemical cells". *Nature*, vol. 414, pp. 338-344. 2001
- [2] H. Wang and J. P. Lewis. "Second-generation photocatalytic materials: aniondoped TiO_2 ". *Journal of Physics: Condensed Matter*, vol. 18, pp. 421-434. 2006
- [3] A. Fujishima and K. Honda. "Electrochemical photolysis of water at a semiconductor electrode". *Nature*, vol. 238, pp. 37-38. 1972
- [4] O. Khaselev and J. A. Turner. "A monolithic photovoltaic-photoelectrochemical device for hydrogen production via water splitting". *Science*, vol. 280, pp. 425-427. 1998
- [5] A. J. Bard and M. A. Fox. "Artificial Photosynthesis: Solar Splitting of Water to Hydrogen and Oxygen". *Accounts of Chemical Research*, vol. 28, pp. 141-145. 1995
- [6] M. Spichiger-Ulmann and J. Augustynski. "Aging effects in n-type semiconducting WO_3 films". *Journal of Applied Physics*, vol. 54, pp. 6061-6064. 1983
- [7] W. Erbs; J. Desilvestro; E. Borgarello; and M. Gratzel. "Visible-light-induced oxygen generation from aqueous dispersions of tungsten(VI) oxide". *Journal of Physical Chemistry B*, vol. 88, pp. 4401-4006. 1984
- [8] H. Ali; N. Ismail; M. S. Amin; and M. Mekewi. "Decoration of vertically aligned TiO_2 nanotube arrays with WO_3 particles for hydrogen fuel production". *Frontiers in Energy*, vol. 12, pp. 249-258. 2018
- [9] I. Shiyonovakaya and M. Hepel. "Bicomponent WO_3/TiO_2 Films as Photoelectrodes". *Journal of Electrochemical Society*, vol. 146, pp. 243-249. 1999
- [10] S. Higashimoto; N. Kitahata; K. Mori; and M. Azuma. "Photo-electrochemical properties of amorphous WO_3 supported on TiO_2 hybrid catalysts". *Catalysis Letters*, vol. 101, pp. 49-51. 2005

- [11] H. Tada; A. Kokubu; M. Iwasaki; and S. Ito. "Deactivation of the TiO₂ photocatalyst by coupling with WO₃ and the electrochemically assisted high photocatalytic activity of WO₃". *Langmuir*, vol. 20, pp. 4665-4670. 2004
- [12] C. S. Fu; C. Lei; G. Shen; and C. G. Yu. "The preparation of coupled WO₃/TiO₂ photocatalyst by ball milling". *Powder Technology*, vol. 160, pp. 198-202. 2005
- [13] J. Engweiler; J. Harf; and A. Baiker. "WO₃/TiO₂ catalysts prepared by grafting of tungsten alkoxides: Morphological properties and catalytic behavior in the selective reduction of NO by NH₃". *Journal of Catalysis*, vol. 159, pp. 259-269. 1996
- [14] S. Eibl; B. C. Gates; and H. Knözinger. "Structure of WO₃/ZrO₂ Catalysts Prepared from Hydrated Titanium Oxide Hydroxide: Influence of Preparation Parameters". *Langmuir*, vol. 17, pp. 107-115. 2001
- [15] H. M. Yang; R. R. Shi; K. Zhang; Y. Hu; A. Tang; and X. Li. "Synthesis of WO₃/TiO₂ nanocomposites via sol-gel method". *Journal of Alloys and Compounds*, vol. 398, pp. 200-202. 2005
- [16] D. Ke; H. Liu; T. Peng; X. Liu; and K. Dai. "Preparation and photocatalytic activity of WO₃/TiO₂ nanocomposite particles". *Materials Letters*, vol. 62, pp. 447-450. 2008
- [17] P. K. Shin and A. C. C. Tseung. "Study of Electrodeposited Tungsten Trioxide Thin Films". *Journal of Materials Chemistry*, vol. 2, pp. 1141-1148. 1992
- [18] X. Z. Li; F. B. Li; C. L. Yang; and W. K. Ge. "Photocatalytic activity of WO_x-TiO₂ under visible light irradiation". *Journal of Photochemistry and Photobiology A: Chemistry*, vol. 141, pp. 209-217. 2001
- [19] J. H. Park; O. O. Park; and S. Kim. "Photoelectrochemical water splitting at titanium dioxide nanotubes coated with tungsten trioxide". *Applied Physics Letters*, vol. 89, pp. 163106-163109. 2006b
- [20] J. Zhao; X. Wang; Y. Kang; X. Xu; and Y. Li. "Photoelectrochemical Activities of W-Doped Titania Nanotube Arrays Fabricated by Anodization". *IEEE Photonics Technology Letters*, vol. 20, pp. 1213-1215. 2008
- [21] M. Xiao; L. Wang; X. Huang; Y. Wu; and Z. Dang. "Synthesis and characterization of WO₃/titanate nanocomposite with enhanced photocatalytic properties". *Journal of Alloys and Compounds*, vol. 470, pp. 486-491. 2009
- [22] E.-I. Yang; J.-j. Shi; H.-c. Liang; and W.-k. Cheuk. "Coaxial WO₃/TiO₂ nanotubes/nanorods with high visible light activity for the photodegradation of 2,3-dichlorophenol". *Chemical Engineering Journal*, vol. 174, pp. 539-545. 2011
- [23] C. Das; I. Paramasivam; N. Liu; and P. Schmuki. "Photoelectrochemical and photocatalytic activity of tungsten doped TiO₂ nanotube layers in the near visible region". *Electrochimica Acta*, vol. 56, pp. 10557-10561. 2011
- [24] C. W. Lai and S. Sreekantan. "Visible light photoelectrochemical performance of W-loaded TiO₂ nanotube arrays: structural properties". *Journal of Nanoscience and Nanotechnology*, vol. 12, pp. 3170-4. 2012
- [25] C. W. Lai and S. Sreekantan. "Incorporation of WO₃ species into TiO₂ nanotubes via wet impregnation and their water-splitting performance". *Electrochimica Acta*, vol. 87, pp. 294-302. 2013a
- [26] C. W. Lai and S. Sreekantan. "Preparation of hybrid WO₃-TiO₂ nanotube photoelectrodes using anodization and wet impregnation: Improved water-splitting hydrogen generation performance". *International Journal of Hydrogen Energy*, vol. 38, pp. 2156-2166. 2013b
- [27] C. W. Lai and S. Sreekantan. "Effect of heat treatment on WO₃-loaded TiO₂ nanotubes for hydrogen generation via enhanced water splitting". *Materials Science in Semiconductor Processing*, vol. 16, pp. 947-954. 2013c
- [28] M. Zhang; C. Yang; W. Pu; Y. Tan; K. Yang; and J. Zhang. "Liquid phase deposition of WO₃/TiO₂ heterojunction films with high photoelectrocatalytic activity under visible light irradiation". *Electrochimica Acta*, vol. 148, pp. 180-186. 2014
- [29] W. H. Lee; C. W. Lai; and S. B. A. Hamid. "One-Step Formation of WO₃-Loaded TiO₂ Nanotubes Composite Film for High Photocatalytic Performance". *Materials*, vol. 8, pp. 2139-2153. 2015
- [30] V. K. Mahajan; S. K. Mohapatra; and M. Misra. "Stability of TiO₂ nanotube arrays in photoelectrochemical studies". *International Journal of Hydrogen Energy*, vol. 33, pp. 5369-5374. 2008
- [31] Z. B. Xie; S. Adams; and D. J. Blackwood. "Effects of anodization parameters on the formation of titania nanotubes in ethylene glycol". *Electrochimica Acta*, vol. 56, pp. 905-912. 2010
- [32] F. ShafiaHoor; V. S. Murulidharan; M. F. Ahmed; and S. M. Mayanna. "Study In The Electrochemical Behavior Of WO₃-Pt Coating: A Cyclic Voltammetric Approach". *IOSR Journal of Applied Chemistry (IOSRJAC)*, vol. 1, pp. 09-14. 2012
- [33] Y. S. Krasnov and G. Y. Kolbasov. "Electrochromism and reversible changes in the position of fundamental absorption edge in cathodically deposited amorphous WO₃". *Electrochimica Acta*, vol. 49, pp. 2425-2433. 2004
- [34] L. J. Minggu; W. R. Wan Daud; and M. B. Kassim. "An overview of photocells and photoreactors for photoelectrochemical water splitting". *International Journal of Hydrogen Energy*, vol. 35, pp. 5233-5244. 2010
- [35] K. Shankar; K. Tep; G. K. Mor; and C. A. Grimes. "An electrochemical strategy to incorporate nitrogen in nanostructured TiO₂ thin films: modification of bandgap and photoelectrochemical properties". *Journal of Physic D*, vol. 39, pp. 2361-2366. 2006
- [36] T. Vogt; P. Woodward; and B. Hunter. "The high-temperature phases of WO₃". *Journal of Solid State Chemistry*, vol. 144, pp. 209-215. 1999

- [37] W. Li; J. Li; X. Wang; J. Ma; and Q. Chen. "Photoelectrochemical and physical properties of WO₃ films obtained by the polymeric precursor method". *International Journal of Hydrogen Energy*, vol. 35, pp. 13137-13145. 2010